

Ratiometric Fluorescence Platform Based on Modified Silicon Quantum Dots and Its Logic Gate Performance

Xiangqian Li,^{†,‡} Zhan Zhou,^{*,||} Cheng Cheng Zhang,[⊥] Yuhui Zheng,[‡] Jinwei Gao,^{§,ⓑ} and Qianming Wang^{*,†,‡,ⓑ}

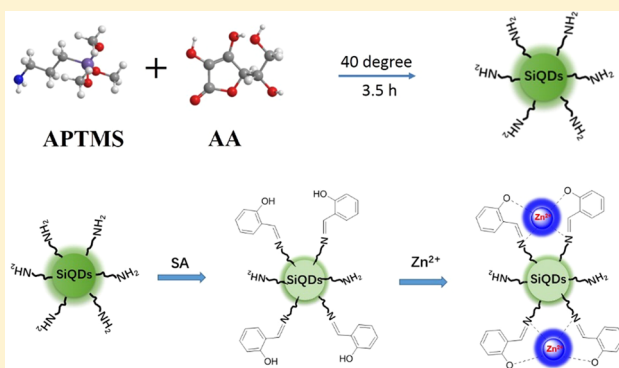
[†]Key Laboratory of Theoretical Chemistry of Environment, Ministry of Education, School of Chemistry & Environment, [‡]School of Chemistry & Environment, and [§]Guangdong Provincial Engineering Technology Research Center For Transparent Conductive Materials, South China Normal University, Guangzhou 510006, China

^{||}College of Chemistry and Chemical Engineering, Henan Key Laboratory of Function-Oriented Porous Materials, Luoyang Normal University, Luoyang 471934, PR China

[⊥]Departments of Physiology and Developmental Biology, University of Texas, Southwestern Medical Center, Dallas, Texas 75390-9133, United States

Supporting Information

ABSTRACT: A novel optical nanoprobe based on silicon quantum dots (SiQDs) has been assembled through a one-pot low-temperature (40 °C) treatment by using 3-(aminopropyl)-trimethoxysilane (APTMS) and ascorbic acid (AA) as two precursors. The water-soluble SiQDs demonstrate intense green luminescence in aqueous environment and the excitation-dependent feature has been explored. Meanwhile, the incorporation of salicylaldehyde (SA) serves to suppress the emission of SiQDs effectively via nucleophilic reaction and an “on–off” change is observed. Furthermore, the addition of Zn²⁺ can lead to evolution of emission peaks, and the green band at 500 nm gradually shifts toward the blue side at 455 nm. The corresponding ratiometric signal changes (I_{455}/I_{500}) can accurately determine the Zn²⁺ concentration and the limit of detection is calculated to be 0.17 μM in the linear range between 1 and 100 μM. In this research, a molecular logic gate (AND) system has been well established by using SA and Zn²⁺ as two inputs. The fluorescence emission changes based on SiQDs will shed new light on the development of functional sensors at the nanoscale level.



INTRODUCTION

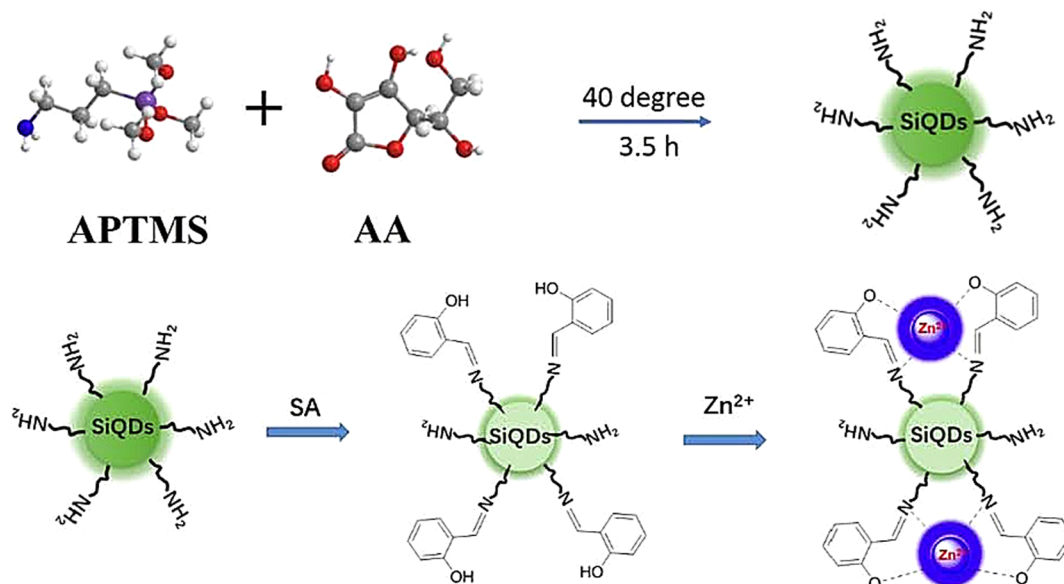
As a newly emerged fluorescent probe, semiconductor quantum dots (QDs) have been widely used in chemo/biosensing field and offer significant advantages over conventional organic molecules and polymeric materials,^{1–3} but the leaching problems of the main elements (such as Pb and Cd) in these nanomaterials will severely restrict their applications. Very recently, fluorescent silicon quantum dots (SiQDs) which are composed of crystalline silicon and oxides have been developed and attracted growing interests owing to their unique properties, such as aqueous solubility, low cost, low cytotoxicity, excitation-dependent multicolor emission, high quantum yield, and high stability against photobleaching.^{4–6} On the basis of these excellent properties, SiQDs have been widely employed as fluorescent probes for detecting a wide range of targets, such as small molecules, ions, and biological macromolecule.^{7–13}

In optical sensor area, functional probes are generally hybrid-type nanomaterials that lie at the interface between the organic chromophores and the hosts. The nanocomposite

materials will provide a variety of opportunities for achieving tailor-made devices due to chemical and physical properties. During the incorporation process, immobilization of the organic frameworks into the accommodating hosts could be realized through different interactions or linkages (including covalent bonds, hydrogen bonds, van derWaals forces, electrostatic interactions, etc.). Lately, the decoration of specific building blocks onto metal–organic frameworks (MOFs) has been reported.^{14,15}

Divalent zinc ions, as the second most abundant metal ion, are distributed in different human tissues, including the brain, intestine, pancreas, and retina.^{16,17} In addition, zinc ions are considered to play critical roles in various physiological and biochemical processes such as apoptosis, gene expression, immune response, and neurotransmission.¹⁸ More importantly, the inconsistency of Zn²⁺ concentration with the normal levels in the human body will cause diverse diseases, such as infantile

Received: March 24, 2018

Scheme 1. Schematic Illustration of SiQDs Synthesis and Zn²⁺ Detection

diarrhea, ischemic stroke, epilepsy, and Alzheimer's disease.¹⁹ The previous mentioned fluorescent chemosensors for Zn²⁺ detection were designed based on quinolone,^{20,21} pyrazoline,²² furan,²³ coumarin,²⁴ BODIPY,²⁵ and other organic fluorophores.^{26,27} However, the exploration of label-free SiQDs as a novel optical analytical platform to monitor Zn²⁺ concentration has never been reported.

As far as the signal response modes are concerned, ratiometric fluorescent chemosensors can exhibit the delicate variation of emission bands upon binding with analytes. Moreover, ratiometric sensing technique possesses several advantages as compared to classical detection methods at a single wavelength since the former is free from errors associated with receptor concentration, photobleaching, and environmental effects. Therefore, it is valuable to exploit functional ratiometric probes with low cost, easy operation, and high selectivity for Zn²⁺ detection. Here, we have assembled a novel SiQDs-based ratiometric fluorescent probe for Zn²⁺ recognition and a "AND" logic gate operation has been provided by using SA and Zn²⁺ as two inputs. First, we have synthesized water-soluble SiQDs by simply mixing and stirring the precursors APTMS and AA. The obtained SiQDs have plentiful amino groups on its surface and exhibit a bright green color emission under UV irradiation. In the presence of SA, the striking luminescence from SiQDs displayed a stepwise decrease due to the electrostatic forces and nucleophilic addition reaction. The aldehyde groups of SA can easily attach to amino groups on SiQDs and finally form SiQDs-SA complex with C=N bonds as linkages. Subsequently, Zn²⁺ can coordinate with SiQDs-SA via imine-N and aromatic-OH from the SA. Consequently, the strong blue emission ($\lambda_{em} = 455$ nm) from the system was observed (Scheme 1). In this way, a facile, fast, and sensitive method for recognizing Zn²⁺ by using silicon-based quantum dots has been well-established.

EXPERIMENTAL SECTION

Reagents and Materials. 3-(Aminopropyl)trimethoxysilane (APTMS 97%) and ascorbic acid (AA, 99.7%) were purchased from Aladdin Chemistry Co., Ltd. All metal salts used were purchased from Guangzhou Chemical Reagent Factory and used without further

purification. All the solutions were prepared with ultrapure water (18.2 M Ω) from a Milli-Q system.

Apparatus. High-resolution transmission electron microscopy (HR-TEM) images were obtained by using a JEOL JEM-2100HR microscope (Japan). UV-vis spectra were recorded on TECHCOMP spectrophotometer in the range of 230–500 nm with a slit of 2 nm. Fluorescence and excitation spectra were measured using a Hitachi F-7000 fluorescence spectrophotometer with a 450 W xenon lamp as a light source. The measurement of decay curves was performed on a FLS920 Edinburgh Instrument (U.K.). X-ray photoelectron spectroscopy (XPS) measurements were performed on a VG ESCALAB 220i-XL surface analysis system. All the experiments were performed at ambient temperature. All error bars represent standard deviations from three repeated experiments. ¹H NMR spectra were recorded on a Bruker Avance 600 MHz NMR Spectrometer. X-ray diffraction (XRD) measurements were performed via a Bruker D8 diffractometer.

Preparation of SiQDs. SiQDs were synthesized by a simple one-step synthesis method from APTMS and AA. Briefly, 10 mL of APTMS was added in 40 mL of ultrapure water within a 200 mL beaker with constant stirring, and the temperature was maintained at 40 °C. Then, 12.5 mL of AA (0.1 M) was added to the above mixed solution by stirring for 0.5, 1.0, 1.5, 2.0, 2.5, 3, or 3.5 h. The SiQDs containing solution was centrifuged at 10 000 rpm for 10 min to remove the large precipitates. For further purifying the SiQDs, the resultant solution was dialyzed in a dialysis bag (molecular weight cutoff = 1000) for 3 days. The resulting SiQDs solution exhibited a bright green color emission under UV irradiation ($\lambda = 365$ nm). The white SiQDs powder was obtained by lyophilization.^{28–30}

Detection of Zn²⁺ in Aqueous Solutions. First, 1 mL of the 0.1 mg/mL as-synthesized SiQDs solution was injected to a spectrophotometer quartz cuvette. Then, 0.3 mM SA and a series of various concentrations of Zn²⁺ were added. The fluorescence spectra were collected after the addition of Zn²⁺ into the solution for 30 s. The photoluminescence spectra were measured by a fluorescence spectrophotometer excited at 367 nm.

RESULTS AND DISCUSSION

Silicon quantum dots have been assembled by one-pot synthesis by using 3-(aminopropyl)trimethoxysilane as a precursor at low temperature. Its microstructure was characterized by transmission electron microscopy (TEM) (Figure 1a). TEM images showed that SiQDs had good monodispersity and spherical shapes of achieved particles were

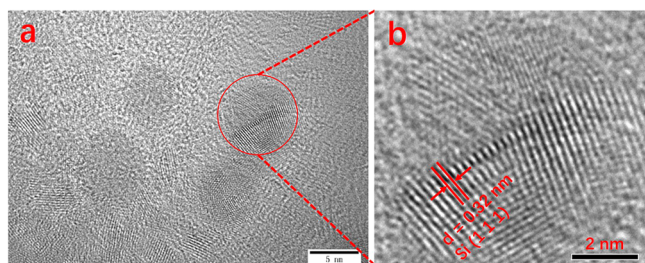


Figure 1. TEM images of the SiQDs (a). HRTEM images of the SiQDs (b). A single QD is enlarged in the inset with a spacing of about 0.31 nm.

confirmed. The average diameter of SiQDs is 7.5 ± 0.5 nm. Additionally, the HR-TEM image of SiQDs demonstrated a crystal lattice with an interplanar distance of around 0.32 nm, which would be ascribed to the (111) lattice plane of crystalline Si₃₀ (Figure 1b). Elemental analysis of the sample by using energy-dispersive X-ray spectroscopy (EDS) indicated that SiQDs were composed of Si, C, O, and N elements (Figure 2a). The additional copper signal was induced by copper grid used in the measurement. Furthermore, the full-scan X-ray photoelectron spectroscopy (XPS) plot of SiQDs was determined to explore their composition and binding energies (Figure 2b). Five peaks, at 103.1, 154.1, 285.1, 399.1, and 530.1 eV, corresponded to Si 2p, Si 2s, C 1s, N 1s, and O 1s, respectively. Figure S1 provided the XRD pattern of SiQDs, and the three signals at 28.4, 47.3, and 56.4° were assigned to (111), (220), and (311) planes of crystalline silicon.

The study of main functional groups and chemical bond structures was performed by analyzing FT-IR spectra. As illustrated in Figure 3, strong absorption bands at 2930 and 2863 cm^{-1} were corresponding to the antisymmetric stretching vibration of the C–H bond.³¹ Two typical bands at 1024 and 744 cm^{-1} were caused by asymmetric vibration and symmetric vibration of Si–O–Si. The strong absorbance at 1665 and 1602 cm^{-1} were assigned to N–H bending vibration.³² Doublet bands located at 3358 and 3291 cm^{-1} were attributed to stretching vibrations of –NH₂ groups from APTMS units, indicating that the coupling agent has been successfully incorporated into the nanosystem.³³ Moreover, the above information demonstrated that quantities of amino groups were covered on the surface of obtained SiQDs.

A valuable property of quantum dots will be their photophysical features and the unique luminescence signal occurs by transitions from electronically excited states to the ground states. In this work, the emission peak of SiQDs was

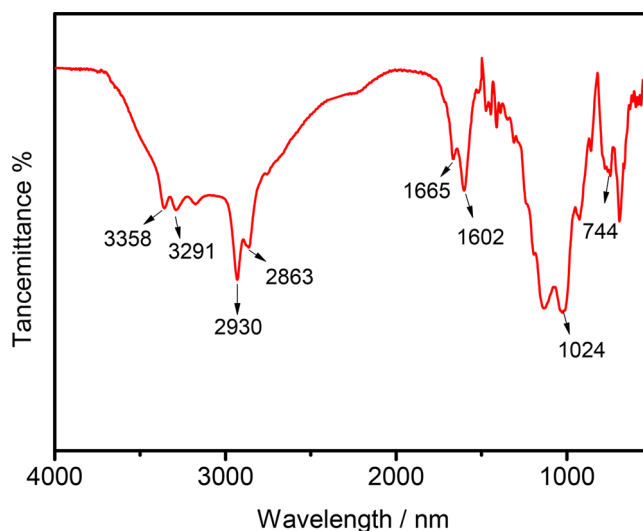


Figure 3. FT-IR spectra of SiQDs.

measured to be situated at 500 nm, and an intense green luminescence was observed upon the excitation at 367 nm (Figure S2). We also investigated the emission curves of the SiQDs at different reaction time (0.5, 1.0, 1.5, 2.0, 2.5, 3.0, and 3.5 h). The collected results displayed that the peak intensity of SiQDs was gradually increased as the reaction hours were extended (Figure S3). Therefore, the experimental condition was optimized at 3.5 h for the preparation of SiQDs in the following studies. In addition, we focused on the effects of different excitation wavelengths on the luminescence of silicon quantum dots. As given in Figure 4, the as-obtained SiQDs exhibited typical excitation-dependent fluorescence behavior. When the excitation wavelength increased from 360 to 510 nm, the emission peak of SiQDs gave rise to red-shifts from 470 to 550 nm. This excitation-dependent fluorescence behavior of SiQDs might be due to the influence of different particle sizes and the wide distribution of various surface trapping states.

It is well-documented that aldehyde groups can easily react with amino groups via the C=N binding Schiff base reaction. The nucleophilic reaction involves the addition of amine to the carbonyl moiety and the elimination of water molecule. After adding SA into the SiQDs solution, its aldehyde groups can accept the attack of the amino groups and imine formation reaction has been carried out. Interestingly, the photoluminescence feature of SiQDs was also changed significantly during this process. In this case, 414 nm was employed as the

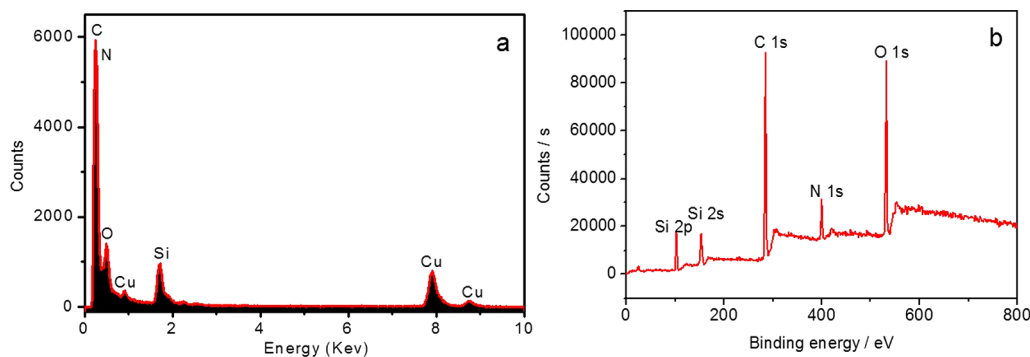


Figure 2. (a) EDS pattern of the SiQDs; (b) XPS spectrum of SiQDs.

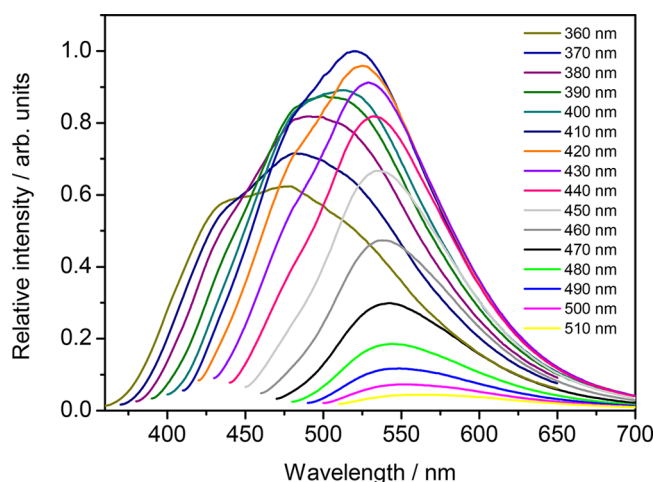


Figure 4. Fluorescence spectra of SiQDs (0.1 mg/mL) at different excitation wavelengths.

excitation wavelength. The visible light sensitization might provide a new choice for blue LED source and direct irradiation of common tissue or biomolecules by ultraviolet lamp could be avoided. Its emission intensity was severely suppressed by the increasing concentration of SA. Finally, the green luminescence was almost quenched upon the addition of 3 mM SA ($\lambda_{\text{ex}} = 414$ nm) (Figure S4A). With the aim of verifying the proposed sensing mechanism, ^1H NMR spectroscopy was applied to explore the nature of the interaction between APTMS and SA. Figure S5 displayed NMR spectral changes of SA in the absence of various equivalents of APTMS. It can be observed that the typical aldehyde proton ($-\text{CH}=\text{O}$) was situated at 11.0. Aromatic $-\text{OH}$ signal was located at 9.91 ppm. Protons in benzene ring were situated at 7.56 and 7.53 ppm. Upon the addition of 0–1 equiv of APTMS to SA, the proton of the aldehyde group at 11.0 ppm disappeared. The aromatic $-\text{OH}$ signal remained almost unchanged. Moreover, a new $-\text{CH}=\text{N}$ group was formed at 8.34 ppm. These results implied that amino groups of APTMS would occur reaction with the aldehyde group of SA via the $\text{C}=\text{N}$ binding Schiff base linkage. The molecular rearrangement and formation of new covalent bond will drastically change the electron distribution. Intramolecular photoinduced electron transfer from donor (amino group) to the aromatic aldehyde unit might result in the emission quenching. On the basis of

luminescence decay curves, the lifetime of SiQDs was 10.9 ns. In the presence of SA, the lifetime was dramatically reduced to 1.8 ns (Figure S6). The results again supported that the covalent attachment of salicylaldehyde would cause intramolecular quenching.

In order to develop a ratio fluorescent probe, we expect that the probe will have detectable fluorescent signals used for recognizing the guest species. In this work, the emission intensity of SiQDs was able to maintain 50% upon adding 0.3 mM SA (Figure S4B). Therefore, 0.3 mM SA was selected for the following detection of Zn^{2+} . The sensing ability of Zn^{2+} based on SiQDs-SA (0.1 mg/mL SiQDs, 0.3 mM SA) has also been studied by the fluorescence spectra. As provided in Figure 5a, in the presence of Zn^{2+} , the green luminescence at 500 nm of SiQDs-SA converted to bright blue color at 455 nm ($\lambda_{\text{ex}} = 367$ nm). Distinguishable changes from green to bright blue color could be observed with the naked eye under irradiation by 365 nm UV light (inset of Figure 5a). As described in Figure 5b, the correlation between the emission change and the concentration of Zn^{2+} followed the excellent linear equation $I_{455}/I_{500} = 0.035x + 0.771$ ($R^2 = 0.999$). The detection of limit (DL) was calculated to be $0.17 \mu\text{M}$ through the equation $\text{DL} = 3 \times \text{SD}/\text{slope}$, where SD is the standard deviation of the blank sample. Parallel experiments were carried out for ten times and the relative standard deviation was calculated to be 1.9%. The detection performance for Zn^{2+} based on a series of analogous materials was summarized in Table S1. It was found that some studies were carried out in organic solvent (DMSO) or organic mixed phases (EtOH/ H_2O). Here the experiment in this research was investigated within pure aqueous environment. Although the detection limit in this study ($0.17 \mu\text{M}$) was not the lowest one, the simultaneous collection of fluorescence signals at two well-resolved wavelengths (ratiometric measurement) would effectively circumvent the problems such as concentration changes of sensors, environmental conditions, and instrument errors. Therefore, the precise quantitative determination could be realized.

Selectivity is another critical point to evaluate the performance of a fluorescent sensor. Hence, the interferences from other ions (Ag^+ , Mg^{2+} , Cd^{2+} , Pb^{2+} , Hg^{2+} , Cu^{2+} , Ca^{2+} , Al^{3+} , Fe^{3+} , PO_4^{3-} , SO_4^{2-} , SO_3^{2-} , HSO_3^- , NO_3^- , NO_2^- , and Cl^-) were investigated under the analogous conditions. As shown in Figure 6, it was observed that other interfering biological ions

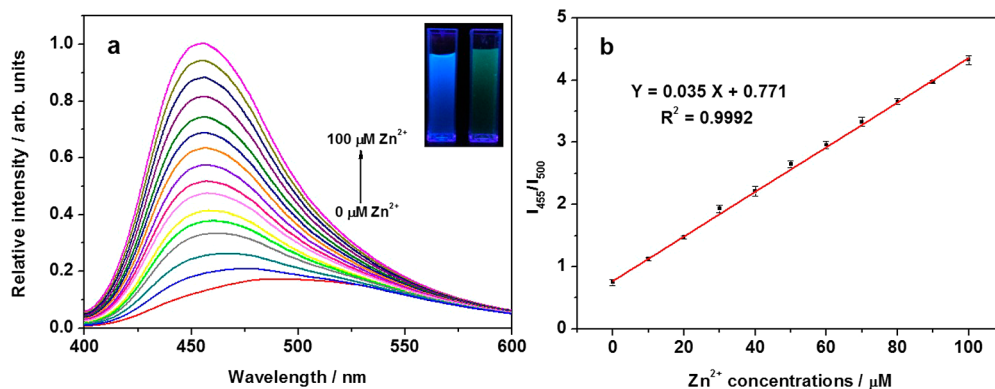


Figure 5. (a) Fluorescence response of SiQDs (0.1 mg/mL) + SA (0.3 mM) in the presence of Zn^{2+} at different concentrations (0, 10, 20, 30, 40, 50, 60, 70, 80, 90, and $100 \mu\text{M}$). (b) linear relationship between the ratio of fluorescence intensities (I_{455}/I_{500}) and Zn^{2+} concentration ($\lambda_{\text{ex}} = 367$ nm).

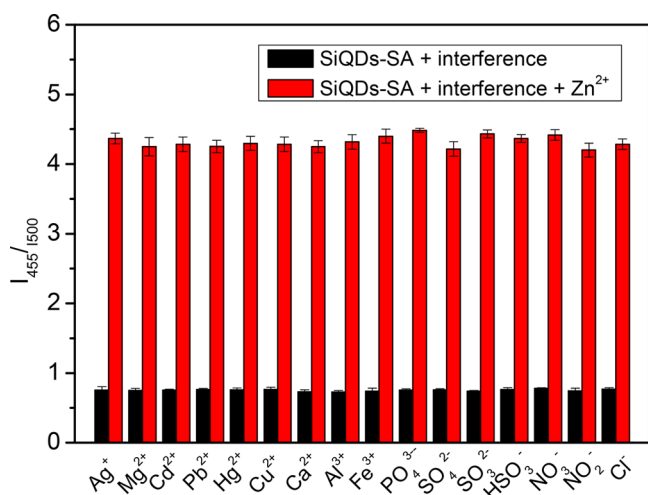


Figure 6. I_{455}/I_{500} of SiQDs (0.1 mg/mL) + SA (0.3 mM) in absence and presence of various substances (1 mM), in the presence (red) and absence (black) of Zn^{2+} (100 μ M), respectively.

exhibited no extraordinary changes on the fluorescence intensity ratio of I_{455}/I_{500} . We also explored the selectivity behavior of the nanoprobe in the presence of a mixture of interference ions (Figure S7). The emission curves showed SiQDs-SA could effectively recognize Zn^{2+} in the mixture of coexisting ions at high concentration (1 mM). These results supported that the SiQD-based nanoprobe was selective for efficient monitoring Zn^{2+} in aqueous solution. In this way, this nanoprobe will be promising in the practical uses in the recognition of metal ions.

Additionally, the feature of reusability of the nanoprobe for the detection of Zn^{2+} ion was explored. Zn^{2+} is able to bind with carboxyl groups of ethylenediaminetetraacetic acid (EDTA) effectively. Accordingly, we studied the emission responses of the nanoprobe to Zn^{2+} by using EDTA as a powerful chelator for metal ions. In Figure S8, the fluorescence intensity ratio was increased in the presence of Zn^{2+} , and it was decreased sharply upon the addition of EDTA. This off-on-off change was observed during five times repeated experiments. Thus, it was deduced that the nanoprobe gave rise to a luminescence response to Zn^{2+} ions and this specific process could be reversible.

In order to clarify the sensing process between the organic building blocks and Zn^{2+} , Job's plot was performed, and their binding stoichiometry toward the target could be determined. In Figure S9, the maximum emission change ($F - F_0$) was found to be situated at 0.34 of molar fraction ratio ($[Zn^{2+}]/[(SA + APTMS) + Zn^{2+}]$), and the analysis result indicated a sensing procedure with binding stoichiometry of 2:1.

The UV-vis spectra of SiQDs, SA, SiQDs-SA, and SiQDs-SA+ Zn^{2+} were recorded. As can be seen in Figure 7, we can hardly observe absorption signals from SiQDs (0.1 mg/mL) in the wavelength range between 230 and 500 nm. In the absorption curve of SA (0.3 mM), two peaks at 245 and 320 nm were identified, which can be attributed to the $\pi-\pi^*$ transition of the aromatic ring structure and $n-\pi^*$ transition of $C=O$. When SA was added into the SiQDs solution, the two absorption peaks shifted to 260 and 387 nm, indicating the amino groups on SiQDs can easily combine to aldehyde groups of SA and SiQDs-SA nanostructure with the $C=N$ Schiff base unit has been formed.³⁴ Upon the addition of Zn^{2+} into the SiQDs-SA solution, the intensity of an absorption

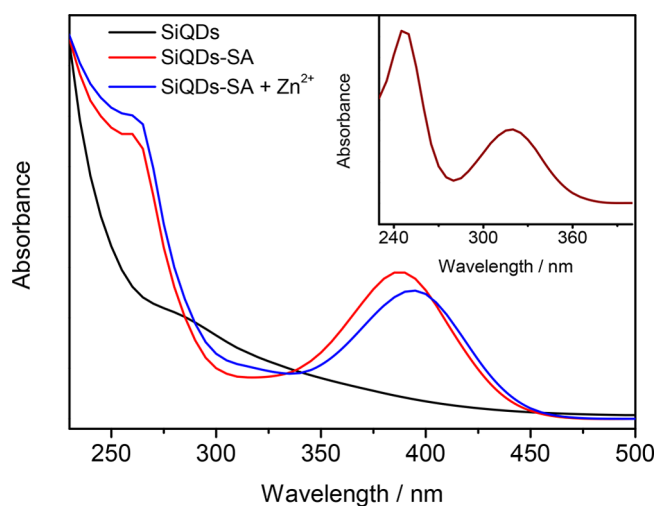


Figure 7. UV-vis absorption spectra of SiQDs (0.1 mg/mL), SA (0.3 mM), SiQDs-SA (SiQDs 0.1 mg/mL; SA 0.3 mM), and SiQDs-SA + Zn^{2+} (SiQDs 0.1 mg/mL; SA 0.3 mM; Zn^{2+} ; 100 μ M). Inset: UV-vis absorption spectra of SA (0.3 mM).

band at 387 nm decreased and its peak wavelength red-shifted to 395 nm. The intensity of absorption signal at short wavelength (260 nm) slightly increased, which also indicated the formation of complexed structure upon coordination of Zn^{2+} with SiQDs-SA via imine-N, and aromatic-OH from the SA moiety.^{35,36} For comparison purpose, Zn^{2+} was directly added into the free SiQDs solution, and there was no any noticeable change in the corresponding UV absorption (Figure S10A). Likewise, Zn^{2+} was also incorporated into the salicylaldehyde solution and the two absorption lines were almost overlapped (Figure S10B). Therefore, this amino-modified SiQDs could be able to develop a typical two-input "AND" logic gate.

It has been reported that molecular logic gates have been employed for mimicking the functions of chemical circuits. Herein, a fluorescent "AND" logic gate could be established by using 0.3 mM SA and 100 μ M Zn^{2+} as the inputs, and the blue signal enhancement ($\lambda_{em} = 455$ nm) as the output. The output values less than a predefined threshold level ($I/I_{max} = 0.5$, I corresponds to the measured emission intensity; I_{max} corresponds to the maximum emission intensity at 455 nm) were referred to binary "0". The emission output values larger than the threshold were defined as binary "1" (Figure 8a). For inputs, the absence and presence of SA or Zn^{2+} was translated into 0 and 1, respectively. For outputs, fluorescence intensity at 455 nm enhancements and none was defined as 1 and 0, respectively. In the absence of either (1/0 and 0/1) or both (0/0) input, no significant changes of blue emission were observed. While in the presence of both (1/1) input, the blue fluorescence was increased enormously. The column bars of the normalized emission intensity and the truth table for the developed "AND" logic gate were given in Figure 8b. Only the system received two inputs together (1/1), the fluorescence signal could be responsive, and the gate was activated and exerted an output signal of "1".

The exploration of these changes according to the logic operation provides direct detection for Zn^{2+} levels. Here, various concentrations of Zn^{2+} (0, 10, 20, 30, 40, and 50 μ M) were selected as the input signals, and the output intensity fluorescent signals were normalized (Figure 9a). As shown in

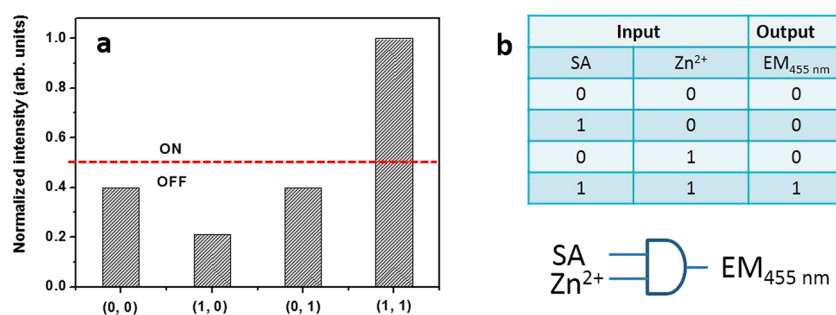


Figure 8. (a) Column diagram of the normalized emission intensity of SiQDs toward 0.3 mM SA and 100 μM Zn^{2+} . (b) Truth table for the developed “AND” logic gate with a two-input logic circuit.

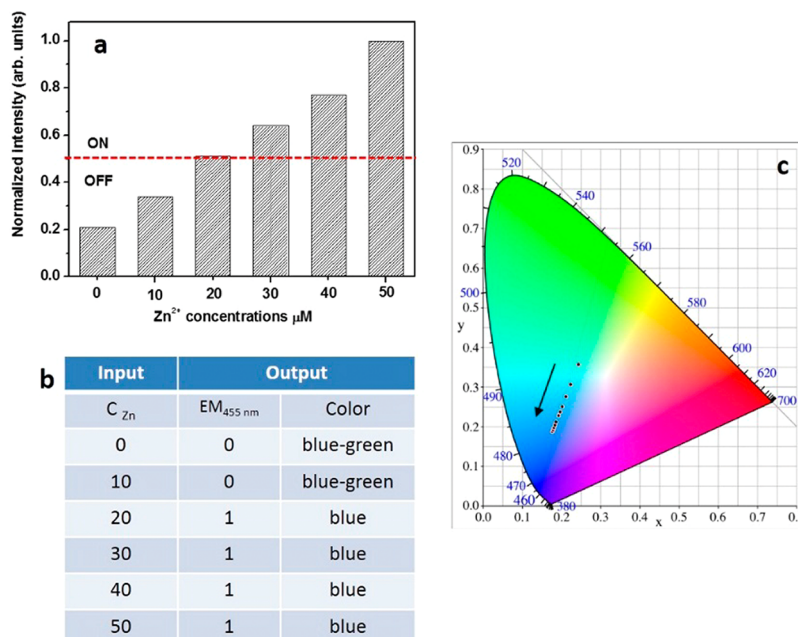


Figure 9. (a) Column diagram of the normalized emission intensity of SiQDs toward 0.3 mM SA and various concentrations of Zn^{2+} (0, 10, 20, 30, 40, and 50 μM). (b) Truth table of the logic analytical device for Zn^{2+} monitoring. (c) CIE chromaticity coordinates of SiQDs at different concentration of Zn^{2+} calculated from the emission spectra shown in Figure 5a.

Figure 9b, 0 gate was triggered by 10 μM Zn^{2+} , and the 1 gate was triggered by 20 μM Zn^{2+} . When the concentration was below 10 μM , the 0 gate emerged. Consequently, the simple binary codes were analyzed for the detection of Zn^{2+} levels. Output 0 represented low concentrations of Zn^{2+} or no Zn^{2+} . The outputs 1 supported the presence of middle or high concentration of Zn^{2+} . On the basis of the detailed investigation, we separated the concentrations (0, 10, 20, 30, 40, and 50 μM) into two groups with their representative colors: 0–10 (blue-green) and 20–50 (blue). In Figure 9c, every concentration of Zn^{2+} has a standard color that can be observed from the CIE calculations using the emission spectra in Figure 5a. In this way, this molecular circuit exhibiting an “AND” logic function will pave a new way for recognizing metal ions based on quantum sized particles.

CONCLUSION

In summary, a label-free fluorescent “AND” logic gate has been developed based on SiQDs for detection of Zn^{2+} . At first, we have synthesized water-soluble SiQDs by mixing and stirring the precursors APTMS and AA under 40 $^{\circ}\text{C}$ for 3.5 h. In the presence of SA, the SiQD-based nanoprobe exhibited

luminescence at 500 nm under UV excitation ($\lambda_{\text{ex}} = 367$ nm). Upon exposure to Zn^{2+} , the nanoprobe displayed a remarkable luminescence color change from green to blue. The intensity ratios (I_{455}/I_{500}) gave rise to a rapid, sensitive and selective response to Zn^{2+} . Moreover, a new “AND” logic gate was designed based on the fluorescent SiQDs for the detection of Zn^{2+} . This work will enable the utilization of unique luminescence properties of SA functionalized SiQDs in medical diagnostics, bioimaging, and environmental monitoring.

ASSOCIATED CONTENT

Supporting Information

The Supporting Information is available free of charge on the ACS Publications website at DOI: 10.1021/acs.inorgchem.8b00788.

XRD pattern of SiQDs; emission spectra of SiQDs with different reaction times; emission spectra of SiQDs in the presence of various concentrations of SA; ^1H NMR spectra of salicylaldehyde (SA, bottom) in the presence of various equivalents of 3-(aminopropyl)-trimethoxysilane (APTMS); table of comparison be-

tween the current study and the reported literatures; interference ions experiments of SiQDs-SA; recycling experiments of SiQDs-SA upon the repeated addition of Zn^{2+} and EDTA; Job's plot for the binding event of L (L refers to the product of salicylaldehyde reacting with 3-(aminopropyl)trimethoxysilane) with Zn^{2+} ions; UV-vis spectra of SiQDs, Zn^{2+} , and SA (PDF)

AUTHOR INFORMATION

Corresponding Authors

*E-mail: zhouzhan@lynu.edu.cn.

*E-mail: qmwang@scnu.edu.cn. Tel.: 86-20-39310258. Fax: 86-20-39310187.

ORCID

Jinwei Gao: 0000-0002-4545-1126

Qianming Wang: 0000-0003-2795-6056

Notes

The authors declare no competing financial interest.

ACKNOWLEDGMENTS

Q.M. acknowledges the support from National Natural Science Foundation of China (grant no. 21371063) and Guangdong Science and Technology plan (2016A050502053). Z.Z. acknowledges the Scientific Research Fund of Henan Provincial Education Department (17A150016) and Natural Science Foundation of Henan (162300410200) for financial assistance. Y.H. thanks the Research Fund of Higher Education Committee of Guangdong Province (GDJ2016003).

REFERENCES

- (1) Pathak, S.; Choi, S. K.; Arnheim, N.; Thompson, M. E. Hydroxylated quantum dots as luminescent probes for in situ hybridization. *J. Am. Chem. Soc.* **2001**, *123*, 4103–4104.
- (2) Mattoussi, H.; Mauro, J. M.; Goldman, E. R.; Anderson, G. P.; Sundar, V. C.; Mikulec, F. V.; Bawendi, M. G. Self-assembly of CdSe-ZnS quantum dot bioconjugates using an engineered recombinant protein. *J. Am. Chem. Soc.* **2000**, *122*, 12142–12150.
- (3) Larson, D. R.; Zipfel, W. R.; Williams, R. M.; Clark, S. W.; Bruchez, M. P.; Wise, F. W.; Webb, W. W. Water-soluble quantum dots for multiphoton fluorescence imaging in vivo. *Science* **2003**, *300*, 1434–1436.
- (4) Wu, S. C.; Zhong, Y. L.; Zhou, Y. F.; Song, B.; Chu, B. B.; Ji, X. Y.; Wu, Y. Y.; Su, Y. Y.; He, Y. Biomimetic preparation and dual-color bioimaging of fluorescent silicon nanoparticles. *J. Am. Chem. Soc.* **2015**, *137*, 14726–14732.
- (5) Ahire, J. H.; Chambrier, I.; Mueller, A.; Bao, Y. P.; Chao, Y. M. Synthesis of d-mannose capped silicon nanoparticles and their interactions with MCF-7 human breast cancerous cells. *ACS Appl. Mater. Interfaces* **2013**, *5*, 7384–7391.
- (6) Li, Q.; He, Y.; Chang, J.; Wang, L.; Chen, H. Z.; Tan, Y. W.; Wang, H. Y.; Shao, Z. Z. Surface-modified silicon nanoparticles with ultrabright photoluminescence and single-exponential decay for nanoscale fluorescence lifetime imaging of temperature. *J. Am. Chem. Soc.* **2013**, *135*, 14924–14927.
- (7) Lin, J. T.; Wang, Q. M. Role of novel silicon nanoparticles in luminescence detection of a family of antibiotics. *RSC Adv.* **2015**, *5*, 27458–27463.
- (8) Ma, S. D.; Chen, Y. L.; Feng, J.; Liu, J. J.; Zuo, X. W.; Chen, X. G. One-step synthesis of water-dispersible and biocompatible silicon nanoparticles for selective heparin sensing and cell imaging. *Anal. Chem.* **2016**, *88*, 10474–10481.
- (9) Zhu, B. Y.; Ren, G. J.; Tang, M. Y.; Chai, F.; Qu, F. Y.; Wang, C. G.; Su, Z. G. Fluorescent silicon nanoparticles for sensing Hg^{2+} and Ag^+ as well visualization of latent fingerprints. *Dyes Pigm.* **2018**, *149*, 686–695.
- (10) Su, Y. Y.; Ji, X. Y.; He, Y. Water-dispersible fluorescent silicon nanoparticles and their optical applications. *Adv. Mater.* **2016**, *28*, 10567–10574.
- (11) Zhang, S. J.; Liu, R. H.; Cui, Q. L.; Yang, Y.; Cao, Q.; Xu, W. Q.; Li, L. D. Ultrabright fluorescent silica nanoparticles embedded with conjugated oligomers and their application in latent fingerprint detection. *ACS Appl. Mater. Interfaces* **2017**, *9*, 44134–44145.
- (12) Luo, L.; Song, Y.; Zhu, C. Z.; Fu, S. F.; Shi, Q. R.; Sun, Y. M.; Jia, B. Z.; Du, D.; Xu, Z. L.; Lin, Y. H. Fluorescent silicon nanoparticles-based ratiometric fluorescence immunoassay for sensitive detection of ethyl carbamate in red wine. *Sens. Actuators, B* **2018**, *255*, 2742–2749.
- (13) Xu, N.; Yuan, Y. Q.; Yin, J. H.; Wang, X.; Meng, L. One-pot hydrothermal synthesis of luminescent silicon-based nanoparticles for highly specific detection of oxytetracycline via ratiometric fluorescent strategy. *RSC Adv.* **2017**, *7*, 48429–48436.
- (14) El-Sewify, I. M.; Shenashen, M. A.; Shahat, A.; Yamaguchi, H.; Selim, M. M.; Khalil, M. M. H.; El-Safty, S. A. Dual colorimetric and fluorometric monitoring of Bi^{3+} ions in water using supermicroporous Zr-MOFs chemosensors. *J. Lumin.* **2018**, *198*, 438–448.
- (15) El-Sewify, I. M.; Shenashen, M. A.; Shahat, A.; Selim, M. M.; Khalil, M. M. H.; El-Safty, S. A. Sensitive and selective fluorometric determination and monitoring of Zn^{2+} ions using supermicroporous Zr-MOFs chemosensors. *Microchem. J.* **2018**, *139*, 24–33.
- (16) Xu, Z. C.; Yoon, J.; Spring, D. R. Fluorescent chemosensors for Zn^{2+} . *Chem. Soc. Rev.* **2010**, *39*, 1996–2006.
- (17) Tomat, E.; Lippard, S. J. Imaging mobile zinc in biology. *Curr. Opin. Chem. Biol.* **2010**, *14*, 225–230.
- (18) Frederickson, C. J.; Koh, J. Y.; Bush, A. I. The neurobiology of zinc in health and disease. *Nat. Rev. Neurosci.* **2005**, *6*, 449–462.
- (19) Noy, D.; Solomonov, I.; Sinkevich, O.; Arad, T.; Kjaer, K.; Sagi, I. Zinc-amyloid β interactions on a millisecond time-scale stabilize non-fibrillar alzheimer-related species. *J. Am. Chem. Soc.* **2008**, *130*, 1376–1383.
- (20) Xu, Y. Q.; Xiao, L. L.; Sun, S. G.; Pei, Z. C.; Pei, Y. X.; Pang, Y. Switchable and selective detection of Zn^{2+} or Cd^{2+} in living cells based on 3'-O-substituted arrangement of benzoxazole-derived fluorescent probes. *Chem. Commun.* **2014**, *50*, 7514–7516.
- (21) Ponnuel, K.; Kumar, M.; Padmini, V. A new quinoline-based chemosensor for Zn^{2+} ions and their application in living cell imaging. *Sens. Actuators, B* **2016**, *227*, 242–247.
- (22) Gusev, A. N.; Shul'gin, V. F.; Meshkova, S. B.; Smola, S. S.; Linert, W. A novel triazole-based fluorescent chemosensor for Zinc ions. *J. Lumin.* **2014**, *155*, 311–316.
- (23) Zhang, T. T.; Wang, F. W.; Li, M. M.; Liu, J. T.; Miao, J. Y.; Zhao, B. X. A simple pyrazoline-based fluorescent probe for Zn^{2+} in aqueous solution and imaging in living neuron cells. *Sens. Actuators, B* **2013**, *186*, 755–760.
- (24) Na, Y. J.; Hwang, I. H.; Jo, H. Y.; Lee, S. A.; Park, G. J.; Kim, C. Fluorescent chemosensor based-on the combination of julolidine and furan for selective detection of zinc ion. *Inorg. Chem. Commun.* **2013**, *35*, 342–345.
- (25) Cao, J.; Zhao, C. C.; Wang, X. Z.; Zhang, Y. F.; Zhu, W. H. Target-triggered deprotonation of 6-hydroxyindole-based BODIPY: specially switch on NIR fluorescence upon selectively binding to Zn^{2+} . *Chem. Commun.* **2012**, *48*, 9897–9899.
- (26) Hirano, T.; Kikuchi, K.; Urano, Y.; Nagano, T. Improvement and biological applications of fluorescent probes for zinc, ZnAFs. *J. Am. Chem. Soc.* **2002**, *124*, 6555–6562.
- (27) Walkup, G. K.; Burdette, S. C.; Lippard, S. J.; Tsien, R. Y. A new cell-permeable fluorescent probe for Zn^{2+} . *J. Am. Chem. Soc.* **2000**, *122*, 5644–5645.
- (28) Li, X. Q.; Gao, J. W.; Rao, S. Y.; Zheng, Y. H. Development of a selective “on-off-on” nano-sensor based on lanthanide encapsulated carbon dots. *Synth. Met.* **2017**, *231*, 107–111.
- (29) Zhou, Z.; Wang, Q. M.; Wang, J. Y.; Zhang, C. C. Imaging two targets in live cells based on rational design of lanthanide organic structure appended carbon dots. *Carbon* **2015**, *93*, 671–680.

(30) Ye, H. L.; Cai, S. J.; Li, S.; He, X. W.; Li, W. Y.; Li, Y. H.; Zhang, Y. K. One-pot microwave synthesis of water-dispersible, high fluorescence silicon nanoparticles and their imaging applications in vitro and in vivo. *Anal. Chem.* **2016**, *88*, 11631–11638.

(31) Wang, J.; Ye, D. X.; Liang, G. H.; Chang, J.; Kong, J. L.; Chen, J. Y. One-step synthesis of water-dispersible silicon nanoparticles and their use in fluorescence lifetime imaging of living cells. *J. Mater. Chem. B* **2014**, *2*, 4338–4345.

(32) Chen, M. H.; Zheng, Y. H.; Gao, J. W.; Li, C.; Yu, C. F.; Wang, Q. M. Fluorometric determination of dopamine by using a terbium (III)inorganic-organic network. *Microchim. Acta* **2017**, *184*, 2275–2280.

(33) Zhou, Z.; Wang, Q. M.; Lin, J. T.; Chen, Y. N.; Yang, C. Q. Nucleophilic addition-triggered lanthanide luminescence allows detection of amines by Eu(thenoyltrifluoroacetone)₃. *Photochem. Photobiol.* **2012**, *88*, 840–843.

(34) Li, Z. Y.; Su, H. K.; Zhou, K.; Yang, B. Z.; Xiao, T. X.; Sun, X. Q.; Jiang, J. L.; Wang, L. Y. Oxo-spirocyclic structure bridged ditopic Schiff base: A turn-on fluorescent probe for selective recognition of Zn(II) and its application in biosensing. *Dyes Pigm.* **2018**, *149*, 921–926.

(35) Anand, T.; Kumar, S. K. A.; Sahoo, S. K. Vitamin B6 cofactor derivative: a dual fluorescent turn-on sensor to detect Zn²⁺ and CN⁻ ions and its application in live cell imaging. *ChemistrySelect.* **2017**, *2*, 7570–7579.

(36) El-Sewify, I. M.; Shenashen, M. A.; Shahat, A.; Yamaguchi, H.; Selim, M. M.; Khalil, M. H.; El-Safty, S. A. Ratiometric fluorescent chemosensor for Zn²⁺ ions in environmental samples using super-microporous organic-inorganic structures as potential platforms. *ChemistrySelect.* **2017**, *2*, 11083–11090.